

A strain-based procedure to estimate strength softening in saturated clays during earthquakes



Chi-Chin Tsai^{a,*}, Lelio H. Mejia^b, Philip Meymand^b

^a Department of Civil Engineering, National Chung Hsing University, Taiwan

^b URS Corporation, 1333 Broadway, Suite 800, Oakland, CA 94612, USA

ARTICLE INFO

Article history:

Received 23 September 2013

Received in revised form

5 July 2014

Accepted 7 July 2014

Keywords:

Clay

Cyclic softening

Earthquake

Strain-based approach

ABSTRACT

Cyclic softening and strength loss of saturated clays during earthquakes is often an important consideration in engineering problems such as slope stability, dam/levee safety, and foundation bearing capacity. This study proposes a simplified procedure for evaluating cyclic softening (amount of strength loss) that may be expected in saturated clays during earthquakes and illustrates how to implement it in engineering analysis. The procedure has two main steps: (1) estimation of an equivalent cyclic shear strain amplitude and associated number of cycles induced in the soil mass by an earthquake; and (2) estimation of softening and strength loss in the soil mass. A key aspect of the proposed procedure is adoption of a strain-based approach to estimate cyclic softening as opposed to the widely used stress-based approach of liquefaction assessments. A threshold strain concept originating from the strain-based approach is first discussed and the development of a procedure is presented subsequently. The proposed procedure provides reasonable, first-order estimates of cyclic softening consistent with the other developed procedures. In addition, the capability of the procedure is demonstrated with two case histories identified as involving cyclic softening of clays.

© 2014 Elsevier Ltd. All rights reserved.

1. Introduction

Cyclic softening of clays is commonly understood as the reduction in soil stiffness and strength due to repeated cyclic loading, as shown in Fig. 1 and discussed in [1]. Experiments by Idriss et al. [2] showed that the initial stiffness and the ordinates of the backbone curve of soft clay are reduced after several cycles. Vucetic and Dobry [3] studied the effect of the overconsolidation ratio (OCR) on the cyclic shear modulus degradation of clay. They found that higher OCR of soil is, less degradation is observed. Matasovic and Vucetic [4] further discussed the coupling of cyclic softening of clay and pore-water pressure generation. With the use of a threshold strain concept, they proposed a model to predict softening behavior based on cyclic shear strain amplitude. More recently, Soroush and Soltani-Jigheh [5] compared pre-cyclic and post-cyclic behavior of mixed clayey soils. The tests results suggest that the post-cyclic undrained shear strength and secant deformation modulus of the specimens are comparatively reduced. The reduction level depends on the granular material content, cyclic shear strain level, and to some degree, the effective confining pressure.

Recent case histories have revealed evidence of cyclic softening of clays during earthquakes. The 1999, Chi-Chi, Taiwan Earthquake caused extensive ground failure and structural damage in Wufeng, Taiwan. Some of the most interesting cases of damage involved ground failure in areas underlain by low plasticity clayey soils [6]. During the 1999 Kocaeli earthquake, in situ deformation measurements at the Carrefour Shopping Center showed significant vertical strains in elastic silt (ML)/lean clay (CL) and fat clay (CH) strata. Martin et al. [7] concluded that the ML/CL layer had exhibited “liquefaction type behavior” while “a definitive explanation for significant earthquake-induced settlements in a high-plasticity clay stratum (CH) in Lot C has not yet been found.” Tsai and Hashash [8] used a novel inverse analysis framework, SelfSim, to extracting the in-situ soil behavior under seismic loading through vertical array recordings in Lotung and La Cienega. The underlying soils exhibit degradation behavior, in which sandy soil is more significant than clayey soil.

Recently, Boulanger and Idriss [9] developed a procedure for evaluating the potential for cyclic softening in clay-like fine-grained soils during earthquakes. Their procedure uses a stress-based approach comparable to that used in semi-empirical liquefaction procedures (e.g. [10]). The procedure is to assess the factor of safety (possibility of onset of significant strains or strength loss) in saturated silts and clays during earthquakes. Mejia et al. [11] applied a procedure similar to the Boulanger and Idriss procedure

* Corresponding author. Tel.: +886 4 2287 2221x323; fax: +886 4 2286 2857.

E-mail address: tsaicc@nchu.edu.tw (C.-C. Tsai).

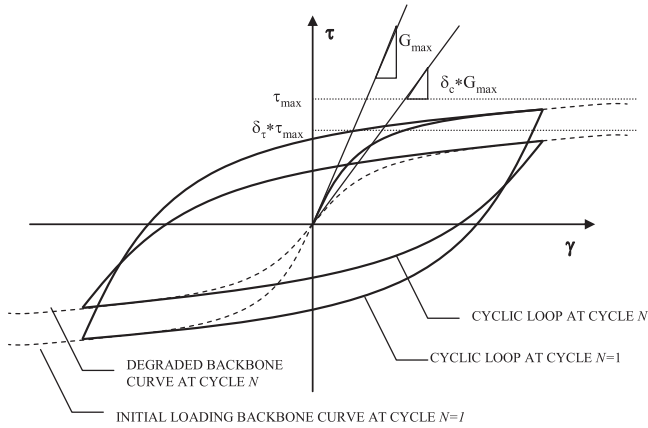


Fig. 1. Illustration of cyclic softening of clays.

Table 1
Model parameters of cyclic softening [4].

OCR	s	r
1	0.075	0.495
1.4	0.064	0.520
2	0.054	0.480
4	0.042	0.423

to estimate post-cyclic strengths of clay-like fine-grained soils and applied it to dam safety evaluation.

This paper, however, proposes a different approach, which uses cyclic shear strain (i.e. strain- based procedure) to evaluate cyclic softening of clayey soils. In addition, unlike [9] to evaluate the onset of soil failure due to cyclic softening, the proposed procedure can directly estimate post cyclic strength and implements it into pseudo static analysis. A threshold strain concept originating from the strain-based approach is first discussed in the paper and the development of a procedure is presented subsequently. Then, the application of proposed procedure is demonstrated by three case studies. It was first compared with another more complex analysis procedure [11] by analyzing the same design case. After that, the procedure is applied to case histories involving strength loss of clayey soils during 1999 Chi-Chi Earthquake and the 1999 Kocaeli earthquake.

2. Threshold strain and strain-based approach to cyclic loading problems

The cyclic threshold shear strain, γ_t , is a key characteristic of the behavior of soils subjected to cyclic loading [12]. According to the definition by Hsu and Vucetic [13], the threshold shear strain amplitude γ_t separates the domains of cyclic pore-water pressure development (or permanent volume change under drained conditions) and practically no development at all. At a cyclic shear strain amplitude, γ_c , larger than γ_t , the residual excess pore-water pressure, Δu , or the volumetric strain, ϵ_v , accumulates continuously with the number of cycles of loading, N_c . Opposite to that, if $\gamma_t < \gamma_c$, such accumulation of Δu or ϵ_v is negligible even for a large N_c . The threshold strain, γ_t , of cohesive soils is usually larger than that of cohesionless soils and it generally increases with the soil plasticity index (PI). For silts and clays having a PI=14–30, $\gamma_t=0.03\text{--}0.06\%$, whereas $\gamma_t=0.01\text{--}0.02\%$ for most sands [13].

The concept of threshold shear strain is an essential component of the so-called cyclic shear strain approach to soil dynamics problems as summarized in [1,14]. In this approach, introduced by

Dobry et al. [15], the cyclic shear strain amplitude is the principal parameter governing changes in the soil microstructure due to cyclic loading. Dobry's approach defined γ_t for pore-water pressure modeling due to cyclic straining of sand. Following the same methodology, Matasovic and Vucetic [4,16] presented cyclic pore-water pressure and softening models for clay that also include γ_t as one of the critical parameters.

3. Cyclic softening models for clay

Matasovic and Vucetic [16,17] proposed a modified hyperbolic model to describe the stress (τ)–strain (γ) behavior (with coupled pore water generation), modulus degradation, and strength softening of clays based on the following equation:

$$\tau = \frac{\delta_c G_{\max} \gamma}{1 + \beta ((\delta_c G_{\max} / \delta_\tau \tau_{\max}) \gamma)^s} \quad (1)$$

where G_{\max} is small strain shear modulus, τ_{\max} is shear strength, δ_c is the modulus degradation index function and δ_τ is the stress softening index function as indicated in Fig. 1. Both indexes are coupled with the excess pore water pressure and are dependent on the soil type. β and s are two curve fitting parameters. For fine-grained clayey soil, the modulus degradation and stress softening indices are equal and can be correlated to the number and amplitude of cycles as follows:

$$\delta_c = \delta_\tau = N_c^{-s(\gamma - \gamma_t)^r} \quad (2)$$

s and r are two curve fitting parameters, which are correlated to clay properties such as plasticity index (PI) and OCR, as listed in Table 1 based on comprehensive laboratory test data [4]. The corresponding cyclic softening model of clays is depicted in Fig. 1. After N_c cycles, the clay presents softening behavior including both strength softening ($\delta_\tau \tau_{\max}$) and modulus degradation ($\delta_c G_{\max}$). Fig. 2 presents an example of strength softening in terms of δ_τ after several numbers of cycles with different cyclic shear strain amplitude for a clayey soil with an OCR of 1. The greater strain amplitude of cycle is, the more softening is expected. Note that only if the cyclic shear strain amplitude is larger than the threshold shear strain, the soil starts to exhibit cyclic softening. In order to quantitatively estimate cyclic softening base on the stress softening index in Eq. (2), the equivalent amplitude of cyclic shear strain and the corresponding number of cycles need to be determined given an earthquake event. In the next two sections, we will discuss how to approximately estimate equivalent amplitude of cyclic shear strain and the corresponding number of cycles from a design earthquake.

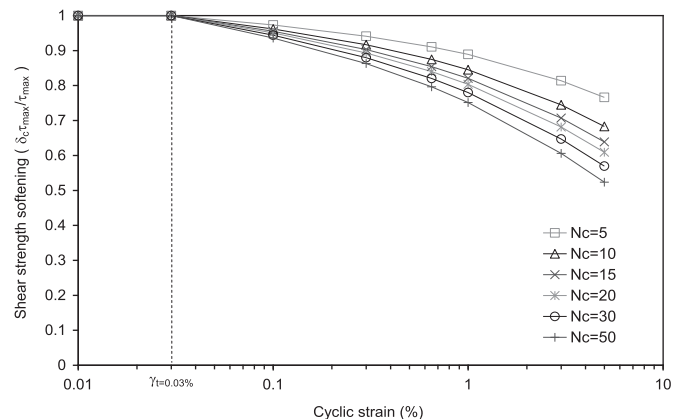


Fig. 2. Strength softening versus cyclic shear strain amplitude and number of cycles.

4. Equivalent cyclic shear strain amplitude

An equivalent (effective) amplitude of cyclic shear strain is first approximated by Tokimatsu and Seed [18] to estimate the seismic compression of unsaturated cohesionless soils. The original Tokimatsu and Seed analysis procedure is based on a simplified representation of the distribution of shear stress with depth in a one-dimensional soil column as proposed by Seed and Idriss [10]. At depth z , the effective cyclic stress, τ_{eff} , can be approximated as

$$\tau_{\text{eff}} = 0.65 \frac{a_{\text{max}}}{g} \sigma_0 r_d \quad (3)$$

where a_{max} is the maximum horizontal ground surface acceleration, g is the acceleration of gravity, σ_0 is the total overburden pressure at depth z , and r_d is a stress reduction factor. Then, the effective shear strain γ_{eff} is estimated from τ_{eff} using the effective shear modulus (G_{eff}) as follows:

$$\gamma_{\text{eff}} = \frac{\tau_{\text{eff}}}{G_{\text{eff}}} = \frac{\tau_{\text{eff}}}{G_{\text{max}}(G_{\text{eff}}/G_{\text{max}})} \quad (4)$$

Combining Eqs. (3) and (4) leads to:

$$\gamma_{\text{eff}} \frac{G_{\text{eff}}}{G_{\text{max}}} = 0.65 \cdot \frac{a_{\text{max}}}{g \cdot G_{\text{max}}} \sigma_0 \cdot r_d \quad (5)$$

The product $\gamma_{\text{eff}}(G_{\text{eff}}/G_{\text{max}})$ in Eq. (5) can be readily translated to a shear strain amplitude γ_{eff} using published models of soil modulus reduction versus shear strain (i.e. models relating γ_{eff} to $G_{\text{eff}}/G_{\text{max}}$) as described latter in this section.

The stress reduction factors originally recommended by Tokimatsu and Seed [18] are the factors proposed by Seed and Idriss [10] that have been widely used for soil liquefaction applications. Several studies (e.g. [19–21]) have proposed recent updates for the factors. Using 2153 combinations of site profiles and input motions, Seed et al. [19] regressed r_d against a_{max} , depth (z), magnitude (M_w), and average soil shear wave velocity in the upper 12 m, and recommended a new relationship for the median of r_d .

The modulus reduction curve may be selected from published models based on index soil properties such as [22,23]. Vucetic and Dobry [22] present the modulus reduction curve as a function of soil plasticity (as represented by PI). Darendeli [23] proposed a family of modulus reduction curves based on a large suite of test results considering the effects of effective confined stress (σ'), PI, and OCR. As an example, Fig. 3 shows a family of modulus reduction curves (based on the [23]) for various PI and OCR under $\sigma' = 100$ kPa. Note that the plots in Fig. 3b are formatted from Fig. 3a, a typical way of presenting modulus reduction curve, to directly estimate shear strain amplitude γ from the product $\gamma(G/G_{\text{max}})$.

5. Equivalent number of uniform strain cycles (N_c)

A large number of studies converted random cycles into equivalent number of uniform strain cycles N_c by using concepts in fatigue studies. Seed et al. [24] first calculated N_c for evaluating liquefaction potential based on the damage accumulation concepts. Using a strong motion data set from tectonically active regions, Liu et al. [25] developed empirical regression equations to evaluate the equivalent number of uniform stress cycles of earthquake shaking as a function of magnitude (M_w), site-source distance, site condition, and near-fault rupture directivity effects. The N_c values were derived based on weighting factors specific to the evaluation of soil liquefaction triggering, which is based on a linear relationship between cyclic stress ratio (CSR) and N_c in

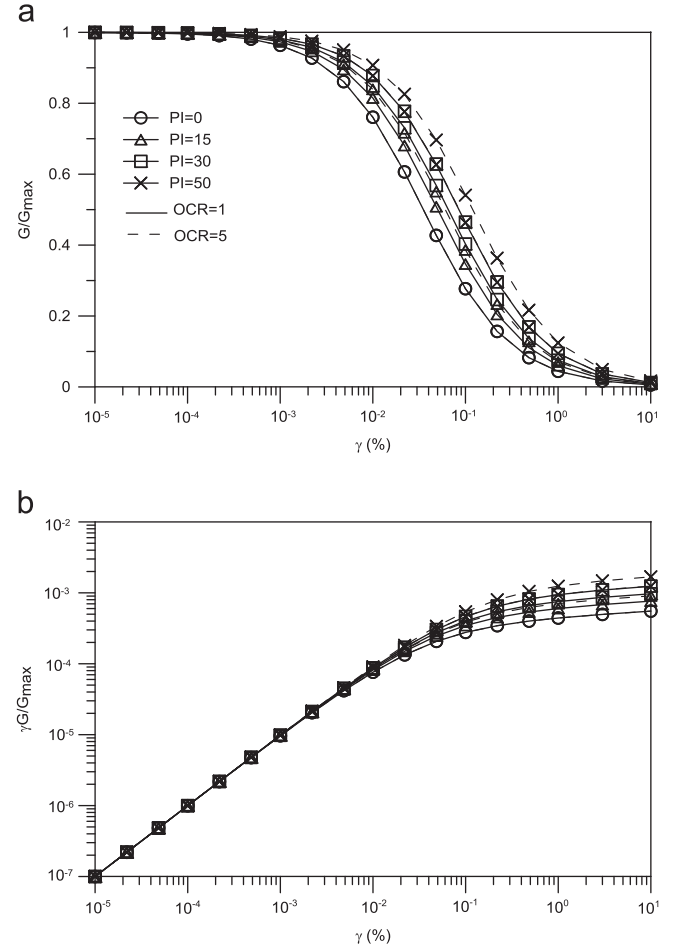


Fig. 3. Modulus reduction curves from [23] re-expressed in the format for estimation of shear strain amplitude.

log-log space established from laboratory tests;

$$\text{CSR} = a \cdot N_c^{-b} \quad (6)$$

where a and b depend on soil property. Typically, b ranges from 0.1 to 0.5 representing clay to sand with respect to liquefaction triggering [9]. In addition, b also depends on the performance (consequences) of analyzed soil column (e.g. amount of accumulated strain/deformation) [26]. The relative number of cycles to cause failure at two different cyclic stress ratios, CSR_A and CSR_B , can be obtained using Eq. (6) as

$$\frac{N_{c,A}}{N_{c,B}} = \left(\frac{\text{CSR}_B}{\text{CSR}_A} \right)^{1/b} \quad (7)$$

Eq. (7) can be used to convert an individual cycle at some stress level to an equivalent number of cycles at a different stress level, by assuming that the “level of damage” is equal for both cases if the numbers of cycles are an equal fraction of the respective number of cycles to failure.

With regard to cyclic softening of clay in the strain approach, the physical meaning of b represents the relative weight of different strain amplitude to cause different levels of softening given an earthquake event. Therefore, Eq. (7) can be re-presented in terms of cyclic shear strain amplitude as below

$$\frac{N_{c,A}}{N_{c,B}} = \left(\frac{\gamma_{c,B}}{\gamma_{c,A}} \right)^{1/b} \quad (8)$$

According to the model by Matasovic and Vucetic [4], b is approximately one given different strength softening conditions in

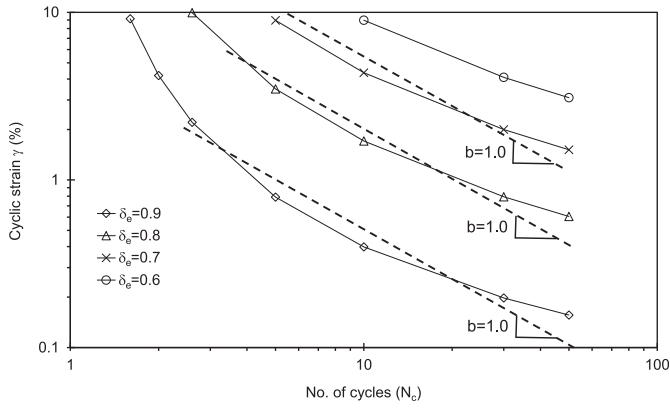


Fig. 4. Relationship between cyclic shear strain amplitude, number of cycles, and modulus degradation index.

terms of δ_c as shown in Fig. 4 where the vertical axis represents cyclic shear strain amplitudes instead of CSR. The solid lines are derived using Eq. (2) given the parameters listed in the Table 1 for OCR=1 and the dashed lines, approximating the solid lines, are obtained with the slope $b=1$ in the log–log space. Therefore, the empirical regression equations by Liu et al. [25] are not applicable for the case of cyclic softening because the weight factors are different due to different b values for different problems.

Kishida and Tsai [27] proposed an empirical equation that can consider different b (weighting factor) values for estimating N_c as below:

$$\ln N_c = \ln \left[\frac{\exp(c_0 + c_1 \ln PGA + c_2 \ln S_1 + c_3 M_w + c_4 \ln b + c_5 b T_s) + 0.5}{0.65^{1/b}} \right] \quad (9)$$

where, $c_0 = -3.43$, $c_1 = -0.352$, $c_2 = -0.402$, $c_3 = 0.798$, $c_4 = 1.72$, and $c_5 = -1.50$. The prediction equation can also estimate N_c at a selected depth (z) by introducing the parameter

$$T_s = \frac{4z}{\bar{V}_s} \quad (10)$$

where \bar{V}_s is average shear wave velocity within depth z based on wave travel time. In addition, the site effect is accounted for by

$$S_1 = \frac{Sa(1.0)}{Sa(0.2)} \quad (11)$$

S_1 is the spectral ratio between 1.0 s spectrum acceleration $Sa(1.0)$ and 0.2 s spectrum acceleration $Sa(0.2)$ and can be obtained from the ground motion prediction equation such as [28]. Kishida and Tsai [27] have shown that their prediction equation can estimate similar N_c as that of Liu [25] for sand ($b=0.35$) at the ground surface. However, the Kishida and Tsai [27] model was originally derived for b values between 0.05 and 0.5. To justify whether the model can be extended to $b=1.0$, the actual value of $\ln(N_c)$ for b values of 0.1–1.0 was manually calculated from a set of 95 motions ($M_w=4.7 \sim 7.4$ and $a_{\max}=0.005 \text{ g} \sim 0.68 \text{ g}$) and compared with the predicted $\ln(N_c)$ by Eq. (9). Fig. 5 shows the residual, defined as the difference between actual and predicted values of $\ln(N_c)$, against different b values. It is clearly shown that the model is unbiased to b values up to 1.0 and thus, can be applied to the cyclic softening problem.

6. Recommended analysis procedure

The procedure to estimate strength softening has two general steps: Step 1 Demand: estimation of the shear strain amplitude and the equivalent number of uniform strain cycles within the soil

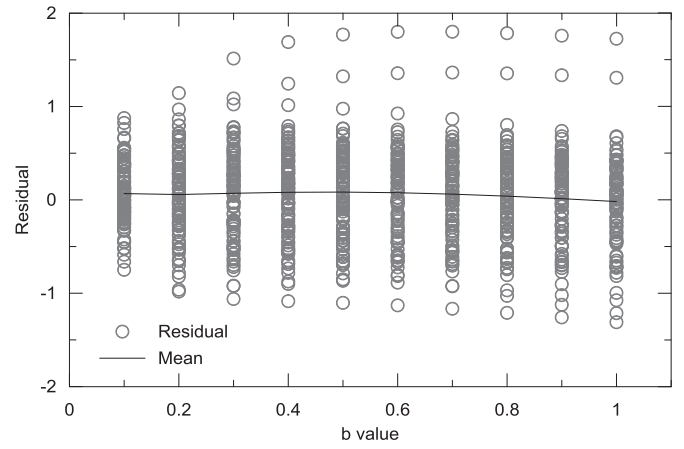


Fig. 5. N_c residual against b value up to 1.0 in the Kishida and Tsai [27] model.

mass from the peak acceleration at the ground surface or other seismological and site parameters; Step 2 Consequence: estimation of strength softening of the soil based on the effective shear strain amplitude, and the equivalent number of uniform strain cycles. Details on the two steps are described in the following:

Step 1 (Demand)

- Estimate the M_w and a_{\max} using appropriate seismic hazard analyses. The a_{\max} value should apply for the ground condition at the surface. This will generally require accounting for ground response effects either through site-specific analysis (preferred) or application of an amplification factor.
 - Measure or estimate the shear wave velocity in the soil profile, and estimate the maximum shear modulus as $G_{\max} = V_s^2 \rho$, where ρ is mass density of soil.
 - Estimate the variation of the product $\gamma_{\text{eff}} (G/G_{\max})$ with depth using Eq. (5).
 - Estimate the effective shear strain amplitude (γ_{eff}) using Fig. 3 or other modulus reduction curves.
 - Estimate the equivalent number of uniform strain cycles, N_c , using Eq. (9)
- If a site specific analysis is performed, step 1(b) to 1(d) can be skipped and γ_{eff} and N_c can be determined directly from the site response analysis output.

Step 2 (Consequence)

- Estimate the soil properties of clay layers where cyclic softening can potentially occur and select the proper parameters from Table 1.
- Estimate δ_c based on calculated γ_{eff} , N_c , and the soil properties using Eq. (2)
- Estimate the cyclic soil strength after cyclic softening by multiplying the strength for 1 cycle by δ_c . The strength for 1 cycle of most clays may be conservatively assumed equal to their static strength.

The estimated softening soil strength can be further used in pseudo-static analysis for the evaluation of slope stability, dam and levee safety, and foundation bearing capacity during earthquakes.

7. Comparison to case histories

In this section, we apply the above analysis procedure to estimate strength softening at three sites during past earthquakes

and compare the predicted consequences due to softening with observed ground failure.

7.1. Berryman reservoir, California, CA, USA

Berryman Reservoir, owned and operated by the East Bay Municipal Utility District, USA, is located in the City of Berkeley in Alameda County, California, and is within the State Alquist-Priolo Earthquake Fault Zone of the Hayward fault. Previous seismic hazard investigations concluded that active traces of the Hayward fault bisect the reservoir. Therefore, for public safety, the reservoir was emptied pending a site-specific fault evaluation. Previous and recent field and laboratory investigations indicated that generally stiff cohesive soils (medium to high PI) grading to highly weathered bedrock are present at the site.

To evaluate the seismic performance of the embankment, URS [29] developed a site-specific design response spectrum and a set of spectra-matched earthquake ground motions for input to the dynamic slope stability analyses. Following the [11] procedure, two-dimensional dynamic response analyses were performed using QUAD4M [30] to estimate the cyclic stresses and accelerations induced by the design earthquake within the reservoir embankment. This comprehensive analysis indicated that the undrained strengths of the saturated clayey soils could be reduced by as much as 40 percent under the post-earthquake condition. Given the same design scenario as listed in Table 2, strength softening was also calculated using the simplified procedure proposed in this paper. It was found that the strengths of the saturated soils could be reduced by approximately 15–20 percent (see Appendix for the detail calculation). Although the predicted strength reduction is less than that by the [11] procedure, it is still a reasonable, first-order estimate of cyclic softening, especially for medium plasticity stiff clay. The yield accelerations (k_y), obtained from pseudo static analyses using UTEXAS4 [31], were 0.16 g for

the pre-earthquake (no strength reduction) and 0.13 g and 0.10 g for post-earthquake condition with 20% and 40% strength softening, respectively. The critical failure plane is shown in Fig. 6.

7.2. Wufeng, Taiwan, 1999 Chi-Chi

The 1999, Chi-Chi, Taiwan Earthquake caused extensive ground failure and structural damage in Wufeng, Taiwan. Liquefaction-induced ground failure occurred in the form of sand boils, lateral spreading, and ground settlement [32]. However, some of the most interesting examples of ground failure occurred in areas underlain by low plasticity clayey soils, in which ground failure was generally not manifest in the free field but only beneath relatively tall, three to six-story, reinforced concrete frame structures with shallow foundations (mats and footings). Results of the analysis by [6] indicated that cyclic softening and associated strength loss in the foundation soils potentially contributed to bearing capacity failures at the edges of the foundation of a six-story building.

According to [6], estimated peak horizontal acceleration of about 0.65 g were produced by the $M_w=7.6$ Chi-Chi earthquake at the site. The six-story building is located approximately 200 m from the fault rupture. Fig. 7 presents the subsurface conditions, which show that a low plasticity silt and clay layer extends across the site. The layer is approximately 3–10 m thick on the east side where the six-story building is located, and approximately 8–12 m thick on the west side. Index tests in the clay layer show PI values ranging from about null to 16. Given the conditions summarized in Table 2, an approximate 30–35% strength loss is estimated in this clay layer (see Appendix A for the detail calculation). According to the [6] estimate considering kinematical interaction effect, load inclination, and the possible range of soil strengths, the factor of safety (FS) for bearing capacity under seismic conditions could range between 1.1 and 2.7 without any strength reduction. If a 30% strength loss is taken into account, the FS for bearing capacity is reduced to 0.8–2.0, which is generally consistent with the field observations that partial bearing capacity failure occurred during the earthquake.

7.3. Carrefour Shopping Center, 1999 Kocaeli

The Carrefour Shopping Center Lot C case history [7] provided a unique set of in situ ground deformation measurements in ML/CL and CH strata from settlement extensometers during the 1999 Kocaeli earthquake, in addition to monitored settlements due to a surcharge of 3.3 m of fill. This case history provides an excellent

Table 2
Summary of input parameters and estimated strength loss of three case histories.

	Seismological information		Site/soil condition			Estimated results			
	M_w (-)	a_{max} (g)	V_s (m/s)	OCR (-)	PI (-)	N_c (-)	γ_{eff} (%)	δ_r (-)	Strength loss (%)
Berryman	7.0	0.72	240	3–5	15–30	18	1–3	0.82	15–20
Wufeng	7.6	0.65	140	1–3	6	20	3	0.68	30–35
Carrefour	7.4	0.24	120	1	10–37	30	0.7	0.81	20

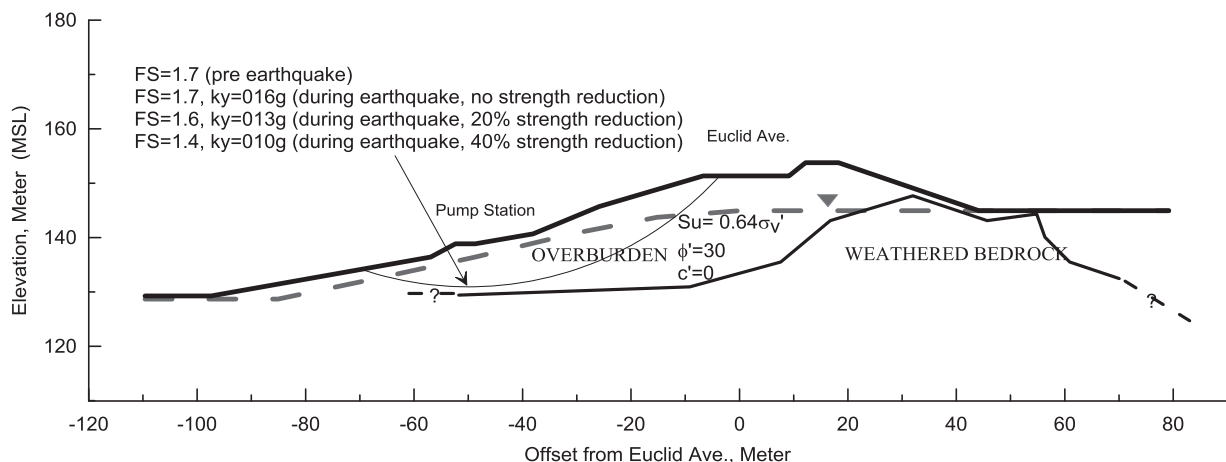


Fig. 6. Pseudo-static analysis considering strength softening at Berryman Reservoir.

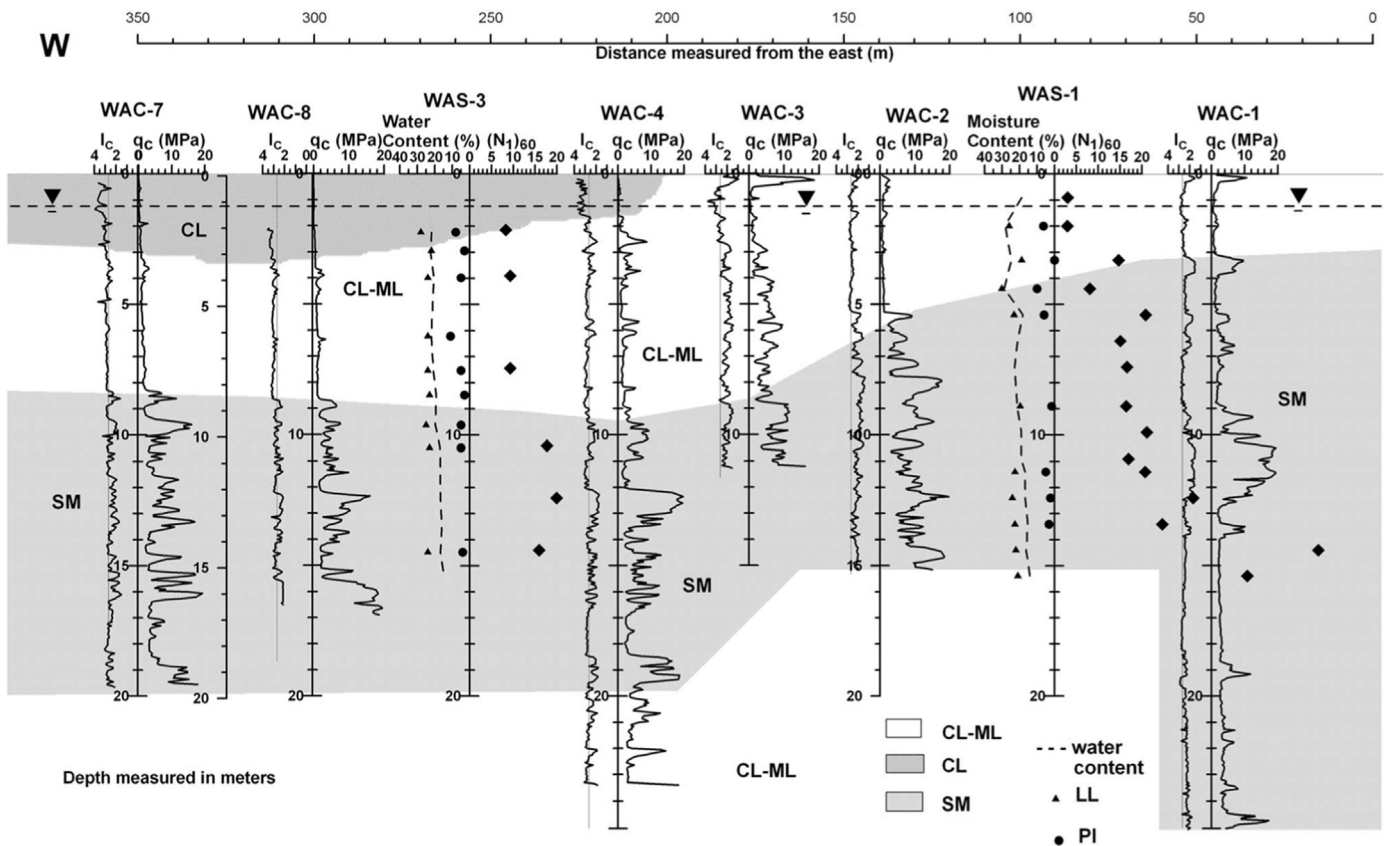


Fig. 7. Subsurface conditions at Wufeng, Taiwan [6].

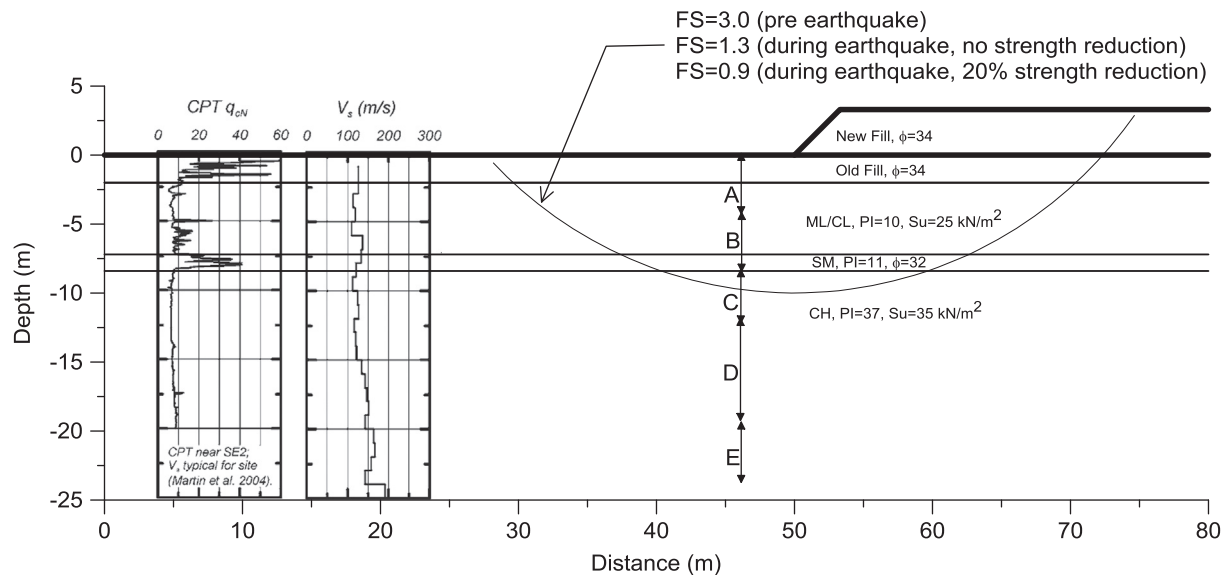


Fig. 8. Subsurface condition at Carrefour Shopping Center, after [7].

example of how fine-grained soils can develop significant strains or failure due to seismic loading, and an opportunity to evaluate the procedures presented herein.

As shown in Fig. 8, the soil profile at Lot C includes a surface layer of approximately 2 m of medium dense fill (gravelly clay, GC), which likely was unsaturated since the water table was at a depth of about 2 m. The next 5 m of soil consists of saturated, soft to firm, low plasticity silt and clay (ML/CL) having average PI values of 10. This layer is underlain by about 1.2 m of loose to medium-dense silty sand, and sand (SP/SM) having an average of 30% fines and a

typical SPT blow count value of about 12. The sand layer is underlain by about 0.9 m of ML/CL soils, followed by medium to stiff, high plasticity clay (CH) that extends to depths greater than 35 m and has average PI values of 37. This lower CH layer becomes much stiffer below a depth of about 25 m.

The vertical strains induced in the fine-grained soil layers by the earthquake are largely attributed to undrained shear deformations beneath the surcharge, as illustrated by Fig. 8. The settlement records in Fig. 9 do show a modest increase in the rate of settlement from just before the earthquake to just after the earthquake. This suggests

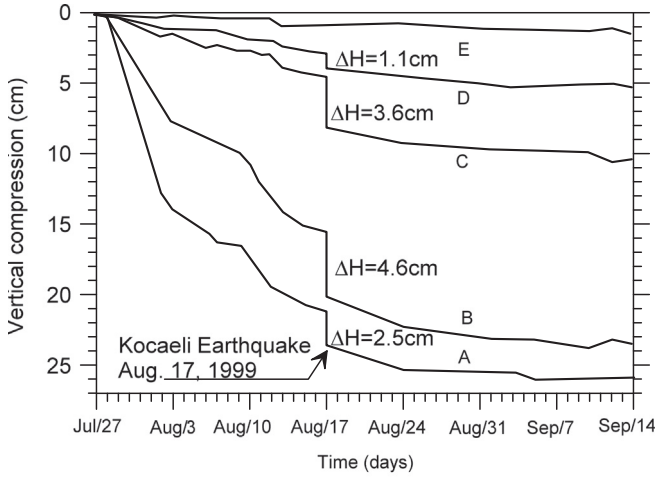


Fig. 9. Extensometer measurements at Carrefour Shopping Center [7].

that the excess pore water pressures shortly after the earthquake were somewhat greater than they were before the earthquake. Nonetheless, it is unlikely that the dissipation of excess pore pressures were the main cause of the observed jumps in settlement on the day of the earthquake. Thus, it is reasoned that the earthquake likely induced moderate excess pore pressures and that the jump in settlements was largely due to undrained shear deformations induced by bearing-capacity mode of deformation.

Bearing-capacity was evaluated in terms of slope stability approach before the earthquake and during the earthquake with pseudo-static type analyses. The failure surface was constrained to a depth of 10 m below the ground surface because the extensometer measurements indicate that large deformation occurred at this depth. As shown in Fig. 8, the FS for slope stability is 3.0 pre-earthquake and becomes less than unit with a 20% estimated strength reduction (see Appendix for the detail calculation),

Appendix A

A.1. Berryman reservoir, California, CA, USA

According to the static analysis (Fig. 6), the depth of critical failure plane is around 10 m. Therefore, 10 m is selected as target depth to evaluate cyclic softening.

Step 1a: see Table 2 for the selected input parameters

Step 1b: $\rho = 2000 \text{ kg/m}^3$, $G_{\max} = 240^2 \times 2000 = 1.15 \times 10^8 \text{ Pa}$

Step 1c: $\gamma_{\text{eff}}(G_{\text{eff}}/G_{\max}) = 0.65 \times (0.72/1.15 \times 10^8)(10 \times 2000 \times 9.8) \times 0.95 = 7.6 \times 10^{-4}$

Step 1d: According to Fig. 3, γ_{eff} is found around 1–3% given $\gamma_{\text{eff}}(G/G_{\max}) = 7.6 \times 10^{-4}$

Step 1e: $T_s = (4 \times 10/240) = 0.17(\text{s})$, $S_1 = (0.3/0.8) = 0.375$ based on design spectrum [29]. Therefore,

$$N_c = \left[\frac{\exp(-3.43 - 0.352 \ln 0.72 - 0.402 \ln 0.375 + 0.798 \times 7.0 + 1.72 \ln 1 - 1.5 \times 1 \times 0.17) + 0.5}{0.65^{1/1}} \right] = 18$$

Step 2a Given $PI = 15$ and $OCR = 3$, $s = 0.048$ and $r = 0.45$. γ_t is assumed as 0.03% for typical clay

Step 2b $\delta_c = 18^{-0.048/(2 - 0.03)^{0.45}} = 0.82$

Step 2c $S_{u, \text{post}} = 0.80 S_{u, \text{static}}$

A.2. Wufeng, Taiwan, 1999 Chi-Chi

The low plasticity silt and clay layer is approximately 3–10 m below the ground surface on the east side where the six-story building is located. Therefore, 3 m is selected as target depth to evaluate cyclic softening.

Step 1a: see Table 2 for the selected input parameters

compared to 1.3 without considering strength loss during the earthquake. The result suggests that the soil layer exhibited strength loss and that the amount of strength loss simply estimated by the proposed procedure leads to an analysis outcome consistent with the field observations.

8. Conclusions

In this paper, we present an analysis procedure to estimate cyclic softening of saturated clays under seismic loading. Unlike common liquefaction potential analysis procedures that use a stress-based approach, the procedure uses a strain-based approach to estimate cyclic softening and associated strength loss. The procedure has two main components: (1) demand: estimation of the shear strain amplitude and the equivalent number of uniform strain cycles within the soil mass induced by an earthquake event; and (2) consequence: estimation of the softening and associated strength loss within the soil given the effective shear strain amplitude and the equivalent number of uniform strain cycles. The procedure is successfully implemented in engineering analysis for analyzing one design case and two field case histories. It is found that the procedure generally provides reasonable, first-order estimates of cyclic softening consistent with field observations for typical clayey soils. For special cases, such as sensitive clay subjected to seismic loading, which can exhibit significant strength loss and large strains, the proposed procedure is not applicable and further investigation and laboratory testing is required.

Acknowledgments

This study was initialized by the first author during his employment with URS Corporation and completed at National Chung Hsing University with the funding from the National Science Council under Award Number NSC102-2625-M-005-004. The authors gratefully acknowledge this support.

Step 1b: $\rho = 1800 \text{ kg/m}^3$, $G_{\max} = 140^2 \times 1800 = 3.52 \times 10^7 \text{ Pa}$

Step 1c: $\gamma_{\text{eff}}(G_{\text{eff}}/G_{\max}) = 0.65 \times (0.65/3.52 \times 10^7)(3 \times 1800 \times 9.8) \times 0.81 = 5.1 \times 10^{-4}$

Step 1d: According to Fig. 3, γ_{eff} is found around 3% given $\gamma_{\text{eff}}(G/G_{\max}) = 5.1 \times 10^{-4}$

Step 1e: $T_s = (4 \times 3/140) = 0.086(\text{s})$, $S_1 = (0.8/1.0) = 0.80$ based on site response analysis [6]. Therefore,

$$N_c = \left[\frac{\exp(-3.43 - 0.352 \ln 0.65 - 0.402 \ln 0.8 + 0.798 \times 7.6 + 1.72 \ln 1 - 1.5 \times 1 \times 0.086) + 0.5}{0.65^{1/1}} \right] = 20$$

Step 2a Given $PI=6$ and $OCR=1$, $s=0.075$ and $r=0.495$. γ_t is assumed as 0.03% for typical clay

Step 2b $\delta_c = 20^{-0.075(3-0.03)^{0.495}} = 0.68$

Step 2c $S_{u, \text{post}} = 0.68 S_{u, \text{static}}$

A.3. Carrefour Shopping Center, 1999 Kocaeli

The failure surface was constrained to a depth of 10 m below the ground surface because the extensometer measurements indicate that large deformation occurred at this depth.

Step 1a: see Table 2 for the selected input parameters

Step 1b: $\rho = 1700 \text{ kg/m}^3$, $G_{\max} = 120^2 \times 1700 = 2.25 \times 10^7 \text{ Pa}$

Step 1c: $\gamma_{\text{eff}}(G_{\text{eff}}/G_{\max}) = 0.65 \times (0.24/2.25 \times 10^7)(10 \times 1700 \times 9.8) \times 0.50 = 5.8 \times 10^{-4}$

Step 1d: According to Fig. 3, γ_{eff} is found around 0.7% given $\gamma_{\text{eff}}(G/G_{\max}) = 5.8 \times 10^{-4}$

Step 1e: $T_s = (4 \times 10/120) = 0.33(\text{s})$, $S_1 = (0.13/0.42) = 0.31$ according to [28]. Therefore,

$$N_c = \left[\frac{\exp(-3.43 - 0.352 \ln 0.24 - 0.402 \ln 0.31 + 0.798 \times 7.4 + 1.72 \ln 1 - 1.5 \times 1 \times 0.33) + 0.5}{0.65^{1/1}} \right] = 30$$

Step 2a Given $PI=15$ and $OCR=1$, $s=0.075$ and $r=0.495$. γ_t is assumed as 0.03% for typical clay

Step 2b $\delta_c = 30^{-0.075(0.7-0.03)^{0.495}} = 0.81$

Step 2c $S_{u, \text{post}} = 0.81 S_{u, \text{static}}$

References

- [1] Ishihara K. Soil behavior in earthquake geotechniques. Oxford: Clarendon Press; 1996.
- [2] Idriss IM, Dobry R, Singh RD. Nonlinear behavior of soft clays during cyclic loading. J Geotechn Eng Div 1978;104:1427–47.
- [3] Vucetic M, Dobry R. Degradation of marine clays under cyclic loading. J Geotech Eng 1988;114:133–49.
- [4] Matasovic N, Vucetic M. Generalized cyclic-degradation-pore-pressure generation model for clays. J Geotech Geoenviron Eng 1995;212.
- [5] Soroush A, Soltani-Jigheh H. Pre- and post-cyclic behavior of mixed clayey soils. Can Geotech J 2009;46:115–28.
- [6] Chu DB, Stewart JP, Boulanger RW, Lin PS. Cyclic softening of low-plasticity clay and its effect on seismic foundation performance. J Geotech Geoenviron Eng 2008;134.
- [7] Martin JJR, Olgun CG, Mitchell JK, Durgunoglu HT. High-modulus columns for liquefaction mitigation. J Geotech Geoenviron Eng 2004;130.
- [8] Tsai C-C, Hashash YMA. Learning of dynamic soil behavior from downhole arrays. J Geotech Geoenviron Eng 2009;135:745–57.
- [9] Boulanger RW, Idriss IM. Evaluation of cyclic softening in silts and clays. J Geotech Geoenviron Eng 2007;133.
- [10] Seed HB, Idriss IM. Simplified procedure for evaluating soil liquefaction potential. J Soil Mech Found Div, ASCE 1971;97:1249–73.
- [11] Mejia L, Wu J, Feldsher T, Yiadom A. Re-evaluation of the seismic stability of Chabot Dam, In: Proceedings of the annual US society on dams conference, USSD 2009, Nashville, TN; 2009.
- [12] Vucetic M. Cyclic threshold shear strains in soil. J Geotech Eng 1992;120:2208–27.
- [13] Hsu C-C, Vucetic M. Threshold shear strain for cyclic pore-water pressure in cohesive soils. J Geotech Geoenviron Eng 2006;132:1325–35.
- [14] Kramer SL. Geotechnical earthquake engineering. Upper Saddle River, NJ: Prentice Hall; 1996.
- [15] Dobry R, Ladd RS, Yokel FY, Chung RM, Powell D. Prediction of pore water pressure buildup and liquefaction of sands during earthquakes by cyclic strain method, In: Proceedings of NBS Building Science Series 138, National Bureau of Standards, Maryland; 1982, p. 150.
- [16] Matasovic N, Vucetic M. Seismic response of soil deposits composed of fully-saturated clay and sand layers, In: Proceedings of the first international conference on earthquake geotechnical engineering, JGS, Tokyo, Japan; 1995, p. 611–6.
- [17] Matasovic N, Vucetic M. Seismic response of composite horizontally-layered soil deposits, UCLA Research report No. ENG-93-182, Civil Engineering Department, University of California, Los Angeles, CA; 1993, p. 452.
- [18] Tokimatsu K, Seed HB. Simplified procedures for the evaluation of settlements in clean sands. Berkely, California: Earthquake Engineering Research Center; 1984.
- [19] Seed RB, Cetin KO, Moss RES, Kammerer AM, Wu J, Pestana JM, et al. Recent advances in soil liquefaction engineering: a unified and consistent framework, In: Proceedings of the 26th annual geotechnical spring seminar, Los Angeles Section of the Geoinstitute, American Society of Civil Engineers, Queen Mary, Long Beach, CA; 2003.
- [20] Idriss IM, Boulanger RW. Soil liquefaction during earthquakes. EERI 2008 (237 pp.).
- [21] Kishida T, Boulanger RW, Abrahamson NA, Driller MW, Wehling TM. Seismic response of levees in the Sacramento-San Joaquin Delta. Earthq Spectra 2009;25:557–82.
- [22] Vucetic M, Dobry R. Effect of soil plasticity on cyclic response. J Geotech Eng 1991;117:87–107.
- [23] Darendeli MB. Development of a new family of normalized modulus reduction and material damping curves, in: Proceedings of the civil engineering, University of Texas at Austin, Austin; 2001, p. 395.
- [24] Seed HB, Idriss IM, Makdisi F, Banerjee. Representation of irregular stress time histories by equivalent uniform stress series in liquefaction analyses. Berkeley: Earthquake Engineering Research Center, University of California; 1975.
- [25] Liu AH, Stewart JP, Abrahamson NA, Moriawaki Y. Equivalent number of uniform stress cycles for soil liquefaction analysis. J Geotech Geoenv Eng 2001;127:1017–1026.
- [26] Onder Cetin K, Bilge H Tolga. Performance-based assessment of magnitude (duration) scaling factors. J Geotech Geoenviron Eng 2012;138:324–34.
- [27] Kishida T, Tsai CC. Seismic demand of the liquefaction potential with equivalent number of cycles for probabilistic seismic hazard analysis. J Geotech Geoenv Eng, ASCE 2014.
- [28] Abrahamson N, Silva W. Summary of the Abrahamson & Silva NGA ground-motion relations. Earthq Spectra 2008;24:67–97.
- [29] Berryman, URS. Reservoir replacement foundation report prepared for East Bay Municipal Utility District, 2008.
- [30] Hudson M, Idriss IM, Beikae M. QUAD4M: a computer program to evaluate the seismic response of soil structures using finite element procedures and incorporating a compliant base. Center for Geotechnical Modeling Department of Civil and Environmental Engineering University of California Davis, Davis California; 1994 (p. 1 v. (various pagings)).
- [31] Wright SG. UTEXAS4-A Computer program for slope stability calculations. Austin, Texas: Shinoak Software; 1999.
- [32] Stewart JP, Chapter 4: Soil liquefaction. Chi-Chi, Taiwan Earthquake of September 21, 1999 Reconnaissance report, Earthquake Spectra, in: Uzarski J, Arnold C, editors, EERI, 2001, p. 17–36.